

FAST IMAGING OF VISIBLE PHENOMENA IN TFTR

R. J. MAQUEDA, G. A. WURDEN
Los Alamos National Laboratory,
Los Alamos, New Mexico,
United States of America

ABSTRACT. A commercial fast-framing visible imaging system was used at the Tokamak Fusion Test Reactor (TFTR) to study edge plasma phenomena. This system was typically operated at 1000 frames/sec with exposures as short as 10 μ s. These short exposures are made possible by the image intensification of the camera, which also allows narrow band interference filters to be used. Sequences of over 1600 digital images (239 pixel \times 192 pixel \times 8 bit) can be captured into temporary memory banks for later slow playback and/or storage into computer archives. Examples are shown illustrating plasma disruption, flying debris, pellet lithium injection, shallow lithium injection (DOLLOP), and edge plasma turbulence. The characteristics of this system makes it also very useful to the machine operator since it provides a slow motion video coverage device interior.

1. INTRODUCTION

In the long-pulse high-temperature magnetically-confined plasma experiments devoted to the development of fusion power, the availability of visible video coverage of the device interior is of great importance for the machine operator. Although the bulk of the power radiated by the plasma in these experiments is at higher photon energies than those in the visible range (typically from the vacuum ultraviolet to the x-ray region), visible emissions are indicative of plasma-wall contacts and consequently related to plasma positioning. The importance of video coverage increases if the system is capable of recording fast events, i.e., time resolution better than the ~ 17 ms of standard video system that operate at 60 fields per second, and can replay these events in slow motion soon after they take place. A further increase in importance is introduced by image intensification since it allows the use of both short exposures and interference filters tuned to different impurity (or fuel) line radiation wavelengths. The fast framing capability together the image intensification turns the system into a useful diagnostic for the physicist looking to study plasma-wall interactions or edge phenomena. In addition, if the imaging system digitizes the images as they are detected (as it probably does to fulfill its slow playback capability), the usefulness of this diagnostic from the physicist's view point increases even further. This diagnostic is then in essence an array of typically over 40000 digitizers with their corresponding detectors and viewing chords that, in principle and if symmetry conditions are met, can be inverted into 2-D emission profiles [1].

In this paper we present a visible imaging system that was used in the Tokamak Fusion Test Reactor (TFTR) [2] during the last one and a half years of operation, and that had all three characteristics mentioned above: fast-framing, intensification, and digital recording. The imaging system, based on a Kodak Ektapro intensified imager coupled to a Kodak

Ektapro EM1012 motion analyzer, was typically operated at 1000 frames per second with exposures as short as 10 μ s. In Section II we present some of the relevant characteristics of the Kodak system as well as of its installation on the TFTR experiment. Employing this fast imaging diagnostic, sequences of digital images were obtained corresponding to different plasma-wall interaction and edge plasma phenomena. In order illustrate the usefulness of the imaging system in the study of these phenomena examples are shown and discussed in Section III.

2. EXPERIMENTAL SETUP

The fast-framing, intensified, digital, visible system is composed of a Kodak Ektapro intensified imager and its controller, a Kodak Ektapro EM1012 motion analyzer [3], and a personal computer for remote control and data storage purposes. The intensified imager is sensitive in the 440-700 nm spectral range, can operate with gates (frame exposures) from 10 μ s to 5 ms, and with full intensifier gain and 1 ms exposure can detect an illuminance of 1.5 lux. The exposure gates are synchronized with the EM1012 motion analyzer processor. This processor digitizes and stores the images in RAM memory for later download to a computer as binary TIF files or slow analog playback. Each full image is composed of 239 \times 192 pixels and the digitalization is 8-bit deep. The motion analyzer in conjunction with the intensified imager can record full images at frame rates ranging from 50 to 1000 frames per second. The system is also capable of running at up to 6000 Hz by splitting the image and rearranging the multiplexing of the digitizers; for example, at the maximum rate only 1/6 of the full image (i.e., 239 \times 32 pixels) can be recorded. The RAM memory available in the system can store up to 1638 full images or the equivalent number of split images, resulting in all cases in a minimum coverage of almost 1.64 s. On the other hand, at any given frame rate, the use of a bigger split factor allows more partial images to be stored in memory and in this way increase the coverage.

Finally, the analog playback can be done as slow as 1 frame (or split) per second.

All of the Kodak equipment was located in TFTR's test cell basement (Fig. 1). The imager itself was mounted on one of TFTR's periscopes beneath the machine, consequently allowing the torus to be viewed from a midplane viewing port [4]. Despite this remote location of the imager respect to the torus, a 3/8" thick soft iron shield had to be used around the imager to reduce the ~600 Gauss magnetic field at the camera location to a level that didn't affect the intensifier. The motion analyzer and the intensifier controller were located 15 feet further away from the torus and closer to the basement floor. A fiber-optic GPIB interface was used across the ~200 m between the Kodak equipment and the control computer that was placed in TFTR's control room annex. The analog video playback from the motion analyzer was also transmitted through a fiber optic to the control room for immediate display after each plasma discharge.

The periscope hardware allowed the use of interference filters placed in a 4 position filter wheel and the selection of the field of view from among three values: 60, 20 and 5 degrees (although only the first two values were used). Among the interference filters employed were: D_{α} , neutral lithium (at 670.8 nm), and singly ionized lithium (at 548.5 nm). The periscope had also full view steering capabilities and a variable aperture. Two examples of digital images are shown in Fig. 2. The image in Fig. 2(a) (obtained with no interference filter, 200 μ s exposure, and 60° field of view) shows the inner bumper limiter of TFTR armored with carbon tiles. The dark, circular cross-section of the torus can be partially observed on the right of the image as well as vertical luminous bands present on the bumper limiter. These vertical bands, where increased recycling takes place, are the consequence of the magnetic field ripple inherent to the 20 toroidal field coils. Hot spots can also be observed on the bumper limiter. A magnified view (20° field of view) of

the bottom end of the bumper limiter is shown in Fig. 2(b). This image was obtained with a Li^+ interference filter at 548.5 nm and 2 ms exposure.

The motion analyzer was generally set to run at framing frequencies between 250 Hz per second (for almost full discharge coverage) and 2 kHz (for fast coverage while still maintaining good spatial resolution) and with the maximum number of pixels allowed by the selected frequency. A full frame rate of 1 kHz was typical. The intensifier's gate and gain were set according to the expected plasma conditions, interference filter used (if any), periscope aperture used, and coating on the viewing port window. This window was blackened due to plasma coatings and radiation damage. While unfiltered operation was possible with exposures down to 10 μs , the use of filters mandated in general exposures no shorter than 200 μs .

The imaging system was remotely controlled from TFTR's control room annex by an Intel based personal computer running either Windows 95 or Windows NT. This computer not only set the intensifier gate and gain but also initialized the motion analyzer into recording mode just before the plasma discharge and retrieved the data once the discharge ended. All processes in the computer were executed under a LabView virtual instrument developed specifically for this application. The analyzer was set into recording mode by the computer when a notification was received from TFTR's DEC cluster through an NFS directory mount. The actual trigger pulse was then given directly to the motion analyzer by TFTR's main control system, CICADA. This pulse indicated the analyzer to either fill in the memory if in pre-trigger mode or to stop refreshing the memory if in post-trigger mode. Once the memory was full with recently acquired frames (or splits) the computer ordered the motion analyzer to start the slow cyclic playback, usually at a rate of 10 frames (splits) per second. The playback lasted until a new notification of an impending discharge was detected, the playback was then stopped and the analyzer

was set in recording mode. This routine was performed by the computer with no user intervention, except for changes in intensifier settings.

Due to the slow GPIB link between the computer and the motion analyzer, retrieval of all digital frames (or splits) was not possible if the following discharge, usually between 8 to 12 minutes later, was to be recorded. At ~ 150 kBd, the rate of frame retrieval is only ~ 25 images per minute. The standard operating procedure was then to always obtain an analog video download to VCR tape during the slow playback and, eventually, perform the digital download of TIF files into the computer's hard disk for only portion(s) of the discharge. The VCR was also controlled automatically through an RS-232 link by the LabView virtual instrument running in the same Intel based computer.

Other magnetically-confined fusion experiments are beginning to use (or plan to use) imaging system such as the one described here. An example is the START spherical torus experiment of UKAEA (Culham) where a faster imaging system, based on a Kodak Ektapro HS4540 imager, is in operation [5]. The START system, although not intensified, is capable of running at a full-frame frequency of 4.5 kHz and a split-frame frequency of up to 40.5 kHz.

3. OBSERVATIONS

Digital images were retrieved directly from the Kodak Ektapro motion analyzer as described in the preceding section. These images were then processed to add the time at which the exposure was obtained respect to the plasma discharge initiation. In this section we show some examples to illustrate the usefulness of the fast-framing imaging system from the physicist viewpoint. Unfortunately, it is not possible to portray here the usefulness from the machine operator's viewpoint, this has to be inferred by the reader from the imaging system characteristics and setup described in Section II. Also, it is not possible to show here sequences of images in movie style, only images placed one besides the other. Due to

this limitation much is lost. Movie style MPEG sequences of the images shown in this paper can be seen through the World Wide Web from the Los Alamos National Laboratory archives at: <http://wsx.lanl.gov/ricky/disrupt.htm>.

Among the phenomena captured on digital images are: plasma disruptions with observation of both precursor activity and aftermath, lithium injection, and edge turbulence. These three phenomena are typified below.

3.1. Disruption-related phenomena

Tokamak plasma discharges sometimes end in sudden losses of equilibrium and confinement, known as disruptions. Some of these disruptions are caused by MHD perturbations that stop rotating with the plasma column, lock on to the wall (i.e., field error) becoming an stationary magnetic perturbation (SMP), and grow in amplitude without saturation [6]. In Fig. 3 a disruption caused by a so called “locked-mode” is shown. The images in this figure were obtained at a sampling rate of 2 kHz with no interference filter and with 30 μ s frame exposure. In Fig. 3(a) the events leading to the disruption can be seen. In this example, a rotating $m=4$ $n=1$ mode (two left-most images) locks on at ~ 2.3 s, plasma-wall contact increases, and triggers the final event, the disruption. The right-most image was obtained during the thermal quench phase.

After the thermal quench, the bulk plasma current is quenched but part of it is briefly transferred to runaway electrons that are created by the strong electric fields present during the disruption. In the example of Fig. 3, a ~ 0.6 MA current remains after the disruption. These high energy (~ 20 MeV) electrons collide against the plasma facing components causing damage. In Fig. 3(b) the damage manifest itself by a (horizontal) shower of debris that “falls” on the top end of the bumper limiter. Although not as spectacular as the example shown here, flying debris are

almost always seen after disruptions. The diameter of the hot-glowing flying particles is estimated to be up to 1 cm and their speed is of the order of 100 m/s. It is speculated that the debris seen in these images is part of the Faraday shield of the RF antenna (IBW) that was located approximately opposite to the section of bumper limiter shown and that was noticed missing a few weeks later.

3.2. Lithium injection

It has been found in TFTR that the injection of lithium by means of pellets positively affected the plasma performance of the tokamak by reducing both fuel recycling and impurity influx from the carbon bumper limiter [8]. Figure 4(a) shows the evolution of one of such injection during a 7 MW neutral beam heated “prelude” of a reverse shear discharge [9]. The lithium pellet is injected at 1.4 s after discharge initiation, producing a short (~ 10 ms) burnthrough spike in the total radiated power. By the end of this spike the fully ionized lithium is escaping the core plasma, recombining in the cooler edge of the torus, where it becomes visible to the fast-framing camera system using a Li^+ interference filter (548.5 nm).

The lithium intensity trace shown in Fig. 4(a) was obtained by observing the emission from one of the vertical, high-recycling bands on the bumper limiter, close to the its top end. After a fast rise, typically of the order of ~ 10 ms, the intensity decays with some fluctuations. For comparison, a 100 ms exponential decay trace has been added to this plot, departures from this decay can be seen to correspond to plasma movements and, consequently, increased recycling. The decay is indicative of how the lithium ions are lost from the core plasma to the cooler edge where the confinement time is substantially lower. We note here that discharges with neutral beam heating, such as the one shown in Fig. 4(a), show a quicker decay of the Li^+ light than discharges with only ohmic heating.

As the lithium diffuses out of the plasma so do excess electrons created during the ionization of the pellet material. The bremsstrahlung radiation from these excess electrons can be observed when no filter is used in the imaging system [Fig. 4(b)]. When the Li^+ interference filter is used, as Figs. 2(b) and 4(a), the radiation from the recycling regions on the top (and bottom) end of the bumper limiter dominate over the bremsstrahlung radiation present in the narrow wavelength-band of this filter.

A new experiment on plasma-wall interaction was performed close to the end of TFTR's operation in which a lithium aerosol was injected into the edge plasma by directing a 30 Hz pulsed YAG laser onto a cup filled with molten lithium. This experiment, termed DOLLOP (Deposition Of Lithium by Laser Outside the Plasma), yielded significant improvements in plasma performance [10]. The characteristics of such a shallow injection of lithium into the plasma can be studied with the fast-framing visible system presented here. Figure 5 shows two example images obtained during the injection of the lithium aerosol. While the individual sub-millimeter aerosol particles can be observed with either a Li^0 filter or no filter [Fig. 5(a)], the use of a Li^+ filter at 548.5 nm allows the ablation cloud that extends toroidally as the lithium enters the edge plasma to dominate [Fig. 5(b)].

Furthermore, the time evolution of the 548.5 nm Li^+ line radiation emission from the edge plasma above the bumper limiter allows the 30 Hz DOLLOP cycle to be observed [Fig. 5(c)]. Each laser discharge is characterized by a fast rise in the Li^+ emission (rise time of 2-3 ms), followed by a slower exponential decay with a characteristic decay time of ~ 9 ms. This Li^+ emission behavior is very similar to that observed close to the DOLLOP source [beginning of the plumes in Fig. 5(b)]. If one then assumes that the source of edge lithium is given by the Li^+ intensity close to the DOLLOP source and considers that the distribution of the lithium along field lines is much faster than 1 ms, then one infers that the life

time of the lithium on the edge of a neutral beam heated plasma has to be much smaller than 9 ms.

3.3. Edge turbulence

Edge turbulent filaments have been previously observed on TFTR using a standard 60 fields/s intensified video camera [11]. These filaments have also been observed with the fast imaging system described in this paper over sections of the inner bumper limiter where there is increased recycling, such as the top edge of the limiter or close to hot spots. In Fig. 6(a) images of the filaments present over the bumper limiter can be seen. These images were obtained during discharge #103782 (with 14 MW of neutral beam heating) with a 20 μ s-long exposure and a 20° field of view. Although no interference filter was used in this example, the edge emission from these filaments is mostly D_α line radiation.

The observed characteristics of these filaments are consistent with those described in Ref. [11]. The fast framing capability of the imaging system allows following the filament evolution at 1 kHz or faster. Although the framing speed of the Kodak system is not enough to follow individual filaments from one frame to another due to their autocorrelation time of less than 150 μ s, some new observations can be made. In the $q \approx 8$ discharge shown, a pellet is injected into the plasma at ~ 3.0 s producing a momentary saturation of the images. Soon after pellet injection, the filaments can not be observed due to either a much shorter autocorrelation time (< 20 μ s) or to their actual suppression by pellet modifications of the plasma profiles. Once the turbulent filaments reappear, the poloidal spacing (i.e., “wavelength”) between filaments is apparently shorter than before the injection. In Fig. 6(b), the wavelength spectra analysis of the turbulent filaments as a function of time can be seen showing also a shift towards shorter wavelengths after the injection of the pellet, decreasing from approximately 9-10 cm to ~ 7 cm.

Furthermore, in the image at 3.0365 s of Fig. 6(a) there is some indication of a very fine structured filament pattern, particularly closer to the midplane, with poloidal spacing smaller than 7 cm.

4. CONCLUSIONS

The fast-framing visible imaging system described in this paper has proven to be quite useful in both machine operation and physics studies. In this paper we have shown examples of plasma disruptions, lithium injection, and edge plasma turbulence where the use of the imaging system leads to new insights on the subjacent physical processes. Given this usefulness, after TFTR ended its operations, we moved the system to the Alcator C-Mod tokamak of the Massachusetts Institute of Technology (MIT).

ACKNOWLEDGMENTS

The authors wish to thank D. O. Whiteson, for his LabView programming, and the TFTR team, in particular G. Lemunyan, D. Long, S. Medley, and C. Bush, for their help in installation, service, and operation of this equipment, and H. Takahashi for the mode analysis. This work was supported by the U.S. DoE under Contracts W-7405-ENG-36 and DE-AC02-76-CH03073.

REFERENCES

- [1] FENSTERMACHER, M. E., MEYER, W. H., WOOD, R. D., NILSON, D. G., ELLIS, R., BROOKS, N. H., Rev. Sci. Instrum. **68** (1997) 974.
- [2] HAWRYLUK, R. J., et al., Phys. Plasmas **5** (1998) 1577.
- [3] Eastman Kodak Company, Motion Analysis System Division, 11633 Sorrento Valley Road, San Diego, CA 92121, USA.
- [4] MEDLEY, S. S., DIMOCK, D. L., HAYES, S., LONG, D., LOWRANCE, J. L., MASTROCOLA, V., RENDA, G., ULRICKSON, M., YOUNG, K. M., Rev. Sci. Instrum. **56** (1985) 1873.
- [5] GATES, D. A., et al., Phys. Plasmas **5** (1998) 1775.
- [6] SNIPES, J. A., CAMPBELL, D. J., HAYNES, P. S., HENDER, T. C., HUGON, M., LOMAS, P. J., LOPES CARDOZO, N. J., NAVE, M. F. F., SCHÜLER, F. C., Nucl. Fusion **6** (1988) 1085.
- [7] TAKAHASHI, H., Fusion Eng. Design **34** (1997) 89.
- [8] TERRY, J. L., et al., in Plasma Physics and Controlled Nuclear Fusion Research (Proc. 13th Int. Conf., Washington, 1990), Vol. 1, IAEA, Vienna (1991) 393.
- [9] SYNAKOWSKI, E. J., et al., Phys. Plasmas **4** (1997) 1736.
- [10] MANSFIELD, D. K., JOHNSON, D. W., KUGEL, H. K., BUSH, C. H., BUDNY, R. V., JASSBY, D., RAMSEY, A., HILL, K., Bull. Am. Phys. Soc. **42**, (1997) 1972.
- [11] ZWEBEN, S. J., MEDLEY, S. S., Phys. Fluids **B1** (1989) 2058.

FIGURE CAPTIONS

Fig. 1. Schematic diagram of the installation of the fast-framing imaging system on TFTR. The Kodak Ektapro hardware in the test cell basement (i.e., intensified imager, intensifier controller, and motion analyzer) was left powered and in running conditions for weeks at a time, if not months, without user intervention.

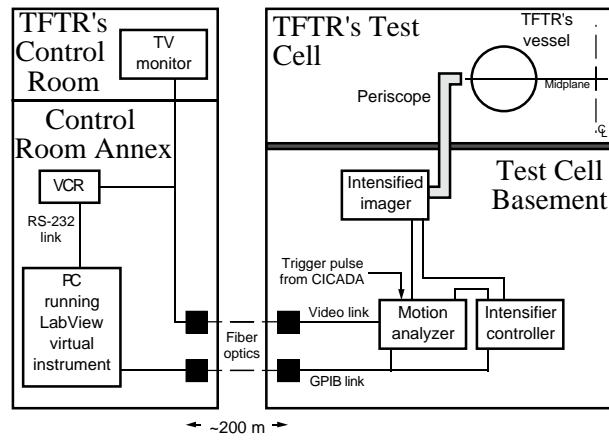
Fig. 2. Examples of digital images: a) Image of the bumper limiter (discharge 93326) obtained with no interference filter, 200 μ s exposure, and 60° field of view. b) Image of the bottom edge of the bumper limiter soon after a lithium pellet was injected (discharge 105223), image obtained with a Li^+ interference filter at 548.5 nm, 2 ms exposure, and 20° field of view. The time references on the images were added a posteriori and not by the motion analyzer processor.

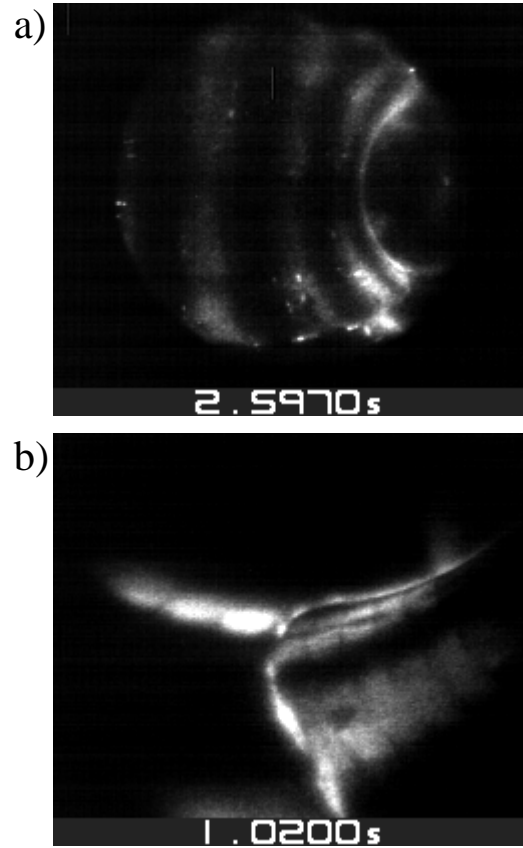
Fig. 3. Disruption caused by a “locked-mode” (discharge 103681). a) Events leading to the disruption: mode rotation, locking, plasma-wall contact, and thermal quench. The time evolution of the plasma current, intensity measured in the region of interest (ROI) indicated in the left most image, and stationary magnetic perturbation (SMP) detector (Ref. [7]) are also shown. b) Flying debris after the disruption (images every 3 ms). These images of the top end of the bumper limiter were obtained with a 20° field of view, no interference filter, and 30 μ s exposure. The carbon tiles on the bumper limiter are typically 10 cm×10 cm in size.

Fig. 4. Lithium pellet injection into TFTR discharges. a) Injection into the 7 MW neutral beam heated prelude of a reverse shear discharge (#96169). The middle plot (Li^+ intensity at 548.5 nm) includes for reference an exponential with 100 ms decay time (dashed line). b) Image of a pellet injected into the tail end of a discharge (#92977) obtained with no interference filter and 100 μ s exposure. The free electrons created during the ionization of the pellet material enhance the bremsstrahlung radiation from the plasma that is observed as a toroid of light.

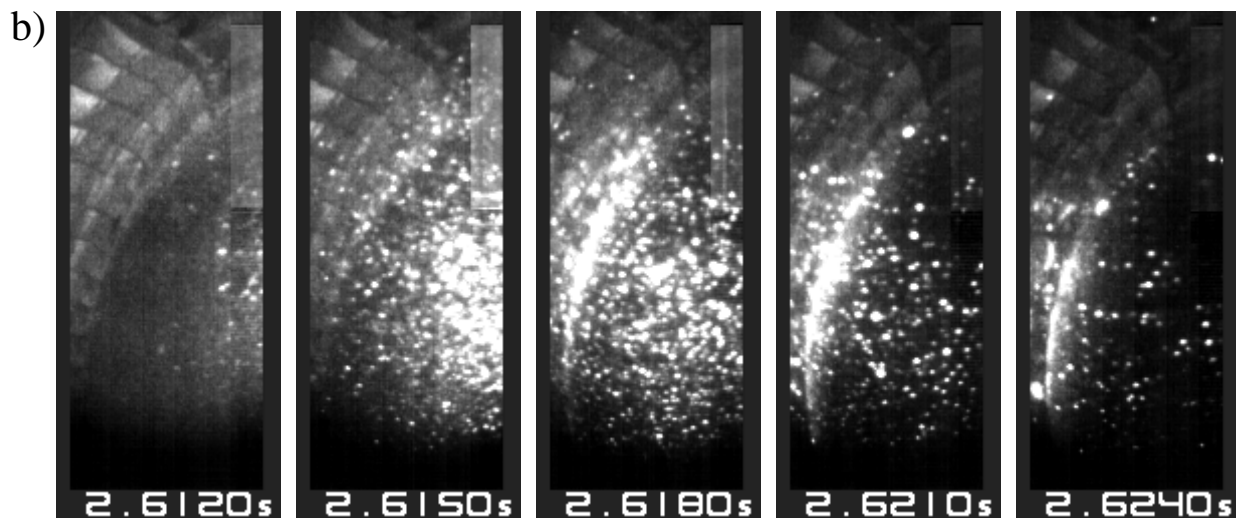
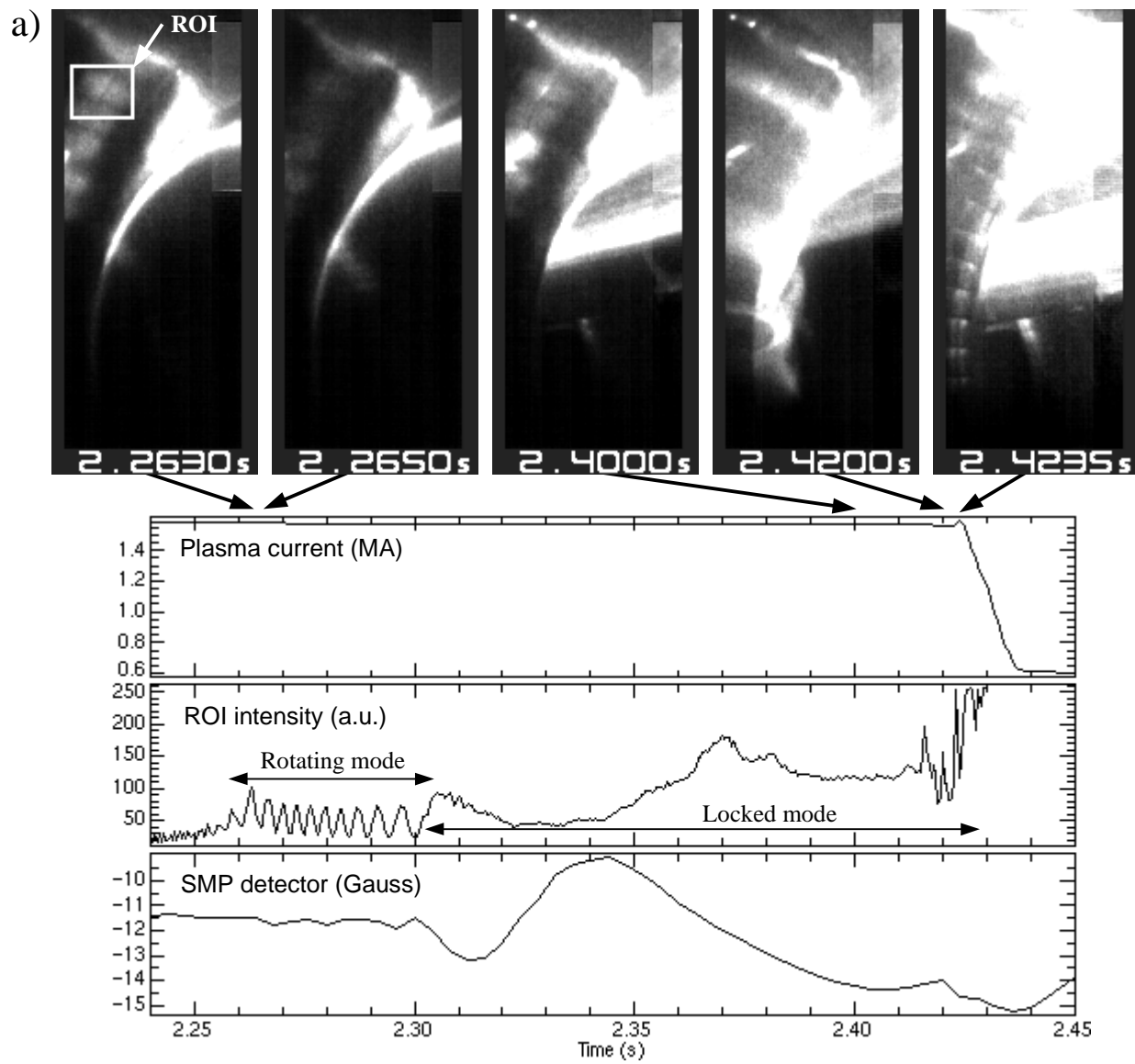
Fig. 5. Shallow lithium injection into neutral beam heated discharges (16-18 MW). a) Image of the aerosol particles (or DOLLOPs) obtained with no interference filter, 30 μ s exposure and 20° field of view (discharge 104023). b) Image of the ablation cloud obtained with a Li^+ interference filter (548.5 nm), 200 μ s exposure and 60° field of view (discharge 104298). The approximate position of the DOLLOP source, the molten lithium cup, is indicated by an asterisk on Figs. (a) and (b). c) Time evolution of the Li^+ intensity during discharge 103618, integrated in a region similar to that indicated in Fig. (b).

Fig. 6. a) Turbulent filaments are observed on the inner bumper limiter with a 20° field of view, 20 μ s-long exposure, and no interference filter. The turbulence is either suppressed by a pellet injected at ~ 3.0 s or their autocorrelation time decreased beyond that discernable with the used exposure. Hot spots on the edges of the carbon tiles can be observed on the images. b) Wavelength spectra analysis of the filaments as function of time: although the filament “wavelength” is poorly defined (i.e., broad spectra), shorter wavelengths can be seen when the filaments reappear after the pellet injection.

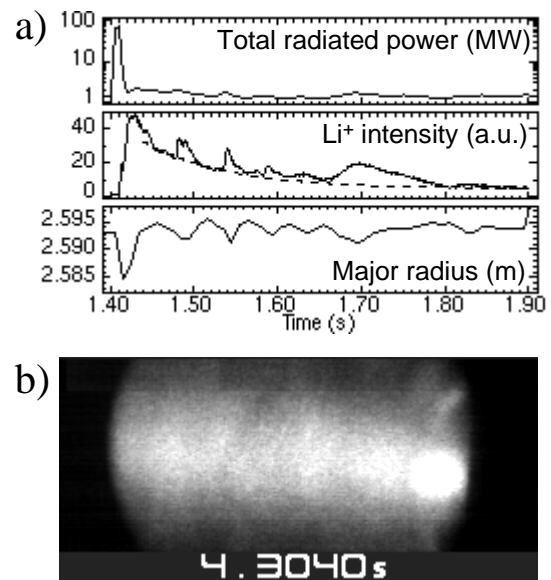




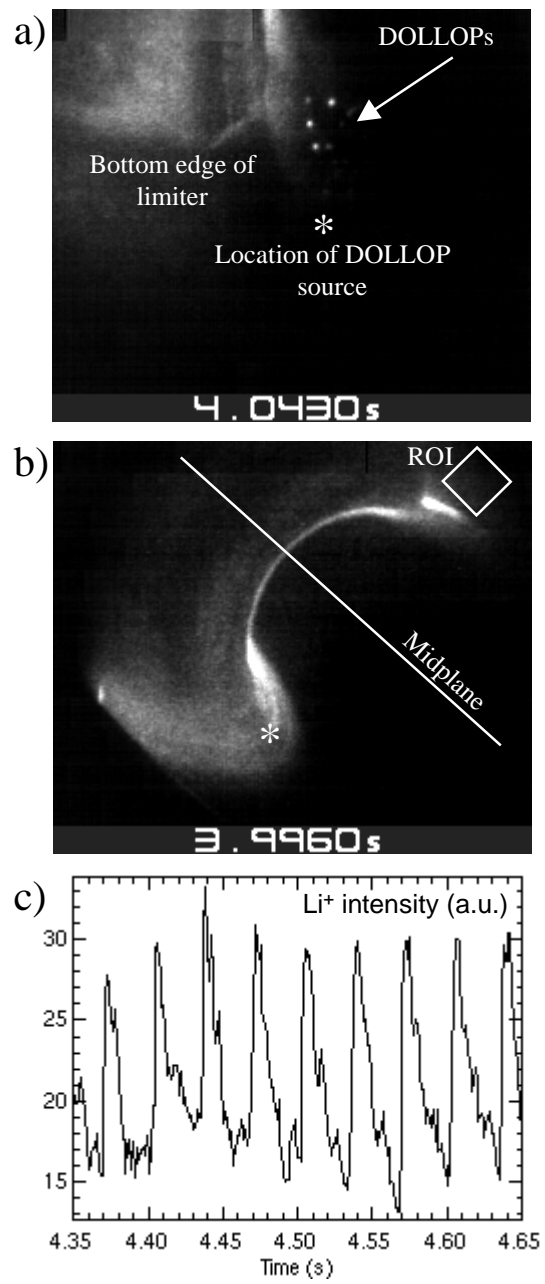
Maqueda and Wurden, Fig. 2



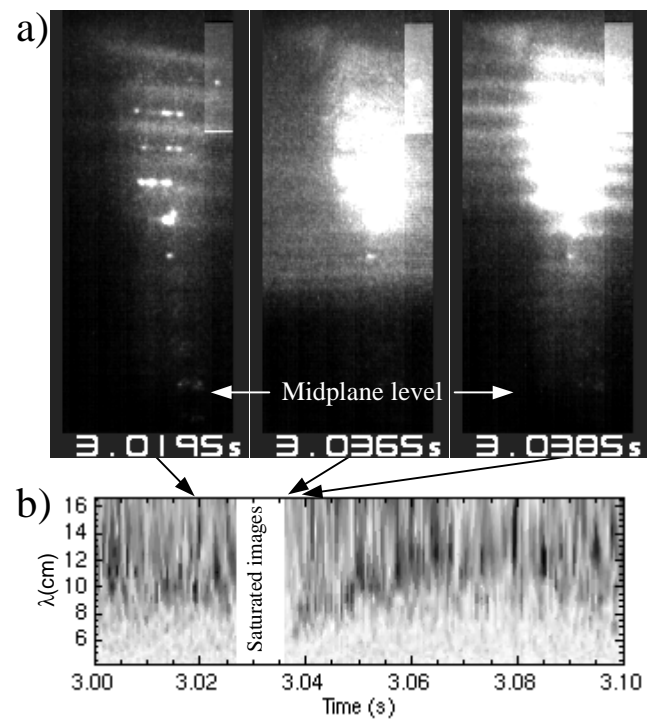
Maqueda and Wurden, Fig. 3



Maqueda and Wurden, Fig. 4



Maqueda and Wurden, Fig. 5



Maqueda and Wurden, Fig. 6